THE JOURNAL OF BIOLOGICAL CHEMISTRY
Vol. 280, No. 19, Issue of May 13, pp. 19146–19155, 2005
Printed in U.S.A.
© 2005 by The American Society for Biochemistry and Molecular Biology, Inc.

S3-12, Adipophilin, and TIP47 Package Lipid in Adipocytes*

Received for publication, January 26, 2005, and in revised form, February 23, 2005
Published, JBC Papers in Press, February 24, 2005, DOI 10.1074/jbc.M500978200

Nathan E. Wolins, Benjamin K. Quaynor, James R. Skinner, Marissa J. Schoenfish, Anatoly Tzekov, and Perry E. Bickel‡

From the Departments of Medicine and Cell Biology & Physiology, Washington University School of Medicine, St. Louis, Missouri 63110

Animals have evolved mechanisms to maintain circulating nutrient levels when energy demands exceed feeding opportunities. Mammals store most of their energy as triacylglycerol in the perilipin-coated lipid droplets of adipocytes. How newly synthesized triacylglycerol is delivered to perilipin-coated lipid droplets is poorly understood. Perilipin is a member of the evolutionarily related family of PAT proteins (Perilipin, Adipophilin, TIP47), which is defined by sequence similarity and association with lipid droplets. We previously showed that S3-12, which is also a member of this family, associates with a separate pool of lipid droplets that emerge when triacylglycerol storage is driven by adding oleate to the culture medium of adipocytes. Our current data extend these findings to demonstrate that nascent lipid droplets emerge with a coat composed of S3-12, TIP47, and adipophilin. After 100 min of oleate treatment, the nascent lipid droplets are more heterogeneous: S3-12 and TIP47 coat smaller, peripheral droplets and adipophilin coats a more medial population of droplets. Fractionation of untreated and oleate-treated adipocytes shows oleate-dependent redistribution of TIP47 and adipophilin from cytosolic fractions to the lipid droplet fraction. Inhibition of protein synthesis with cycloheximide does not block the oleate-induced formation of the nascent lipid droplets, nor does it prevent TAG accumulation. We suggest that the non-lipid droplet pools of S3-12, adipophilin, and TIP47 constitute a ready reservoir of coat proteins to permit rapid packaging of newly synthesized triacylglycerol and to maximize energy storage during nutrient excess.

The ability to store energy as triacylglycerol (TAG)[1] and later mobilize energy from this reservoir as free fatty acids and glycerol allows animals to survive prolonged periods of fasting. Higher animals store TAG in specialized cells, adipocytes, which are able to efficiently synthesize TAG from fatty acid and glucose and package TAG into large storage droplets (10–100-μm diameter). Other cell types have a more limited capacity to store TAG and rarely accumulate large lipid droplets. The robust ability of the adipocyte to store TAG is not without limit. It has been hypothesized that, when the visceral adipose tissue depot fills up, excess lipid "overflows" into other tissues that are less able than adipocytes to package and store TAG. Fatty acids not esterified to glycerol are toxic even at low concentrations (1). In fact, failure to efficiently sequester lipid into the lipid storage droplets of adipocytes has been implicated in the pathogenesis of insulin resistance, nonalchoholic fatty liver disease, β-cell failure, and cardiomyopathy (2).

Little is known of mechanisms by which cells, and adipocytes in particular, package newly synthesized TAG into storage droplets (3, 4). The structure of intracellular lipid droplets is similar to that of lipoproteins, a neutral lipid core is surrounded by a phospholipid monolayer and a protein coat. This structural organization is conserved among animals, plants, and yeast. A likely candidate location for the initiation of lipid droplet biogenesis would be the site of the final step in TAG synthesis. However, the sites of neutral lipid synthesis are unclear. TAG is synthesized from diacylglycerol and fatty acyl-CoA substrates in a reaction catalyzed by acyl-CoA:diacylglycerol acyltransferase (DGAT). At least 2 proteins (DGAT1 and DGAT2) with DGAT activity have been reported. Evidence has been presented that DGAT1 and acyl-CoA:cholesterol acyltransferase (ACAT), the enzyme responsible for steryl ester synthesis, resides in the endoplasmic reticulum (ER) (5, 6). However, the subcellular location of DGAT2 has not been established. These enzymes may not be the only sources of intracellular neutral lipids. Also, the origin of the phospholipid monolayer is not known. Finally, although a number of lipid droplet surface proteins have been reported, how proteins target to and associate with the lipid droplet is not understood.

Based upon biochemical and morphological data primarily in yeast and plants, a prevailing model of lipid droplet formation has emerged. According to this model, neutral lipid is synthesized within the leaflets of the ER membrane bilayer. As neutral lipid accumulates and coalesces within the bilayer, the bilayer distends locally into a "lens" of neutral lipid surrounded by a phospholipid monolayer. Eventually, the lens buds off into the cytosol as a nascent lipid droplet or may remain associated with the ER. This model allows for several mechanisms by which lipid droplet coat proteins might associate with the droplet surface (4). First, coat proteins may reside on the ER membrane and partition with the nascent droplet during lens formation and droplet budding. Second, coat proteins, either as soluble proteins or vesicle-associated proteins may target to the surface of droplets by specific peptide sequences or by hydrophobic interactions. Third, coat proteins may exist as preformed complexes into which newly synthesized neutral lipid is transferred.

In mammals the Perilipin-Adipophilin-TIP47 (PAT) family

* This work was supported by a research award from the American Diabetes Association (to P. E. B.) and National Institutes of Health Grant T32 DK07296 (to N. E. W.). The costs of publication of this article were defrayed in part by the payment of page charges. This article must therefore be hereby marked "*advertisement*" in accordance with 18 U.S.C. Section 1734 solely to indicate this fact.

‡ To whom correspondence should be addressed: Depts. of Medicine and of Cell Biology & Physiology, 660 S. Euclid Ave., Campus Box 8127, St. Louis, MO 63110. Tel.: 314-747-3979; Fax: 314-362-7641; E-mail: pbickel@im.wustl.edu.

[1] The abbreviations used are: TAG, triacylglycerol; BSA, bovine serum albumin; DGAT, acyl coenzyme A:diacylglycerol acyltransferase; ER, endoplasmic reticulum; OGI, oleate, glucose, and insulin; PAT, Perilipin ADRP and TIP47; TIP47, tail-interacting protein of 47 kDa; PBS, phosphate-buffered saline; DIC, differential interference contrast; TEM, transmission electron microscopy.

This paper is available on line at http://www.jbc.org

This is an Open Access article under the CC BY license.

of proteins (7) has been shown to coat lipid droplets. This protein family is defined by lipid droplet binding and sequence similarity. Perilipin and adipophilin (also known as adipocyte differentiation-related protein, ADRP) have been reported to bind to lipid droplets independent of metabolic state; whereas, TIP47 only binds lipid under specific metabolic conditions (8). S3-12 shares sequence similarity with TIP47 and adipophilin and, like TIP47, only coats lipid droplets under certain metabolic states (9). Because these protein sequences are similar to perilipin and can be found at the interface of the lipid droplet with the cytosol, we hypothesize that they organize the packaging and trafficking of intracellular neutral lipid.

Under basal conditions, 3T3-L1 adipocytes have a single population of lipid droplets that are coated by perilipin and tend to cluster around the nucleus, but S3-12 is distributed throughout the cytoplasm in a punctate pattern. We have previously shown that when TAG synthesis is driven by incubating adipocytes in medium supplemented with albumin-bound oleate, a pool of small S3-12-coated lipid droplets emerges at the adipocyte periphery (9). During the first hour of accelerated TAG synthesis, the S3-12-coated lipid droplets remain separate from the perinuclear, perilipin-coated droplets. However, after longer treatment times, the S3-12-coated lipid droplets become larger and are found closer to the nucleus. Longer treatment times also result in a ring of droplets positioned between the peripheral S3-12-coated droplets and perinuclear perilipin-coated lipid droplets that are coated with both proteins. Finally, when adipocytes are removed from the conditions that drive TAG synthesis, S3-12 returns to its more diffuse distribution, leaving only perilipin-coated lipid droplets (9). To extend these observations, we have observed the dynamic process of lipid droplet formation in live adipocytes by differential interference contrast (DIC) microscopy, investigated the ultrastructural features of nascent lipid droplets by transmission electron microscopy (TEM), and determined the integrated behavior of PAT family proteins during accelerated TAG synthesis by fluorescence microscopy. These studies reveal a spatially and temporally ordered process of lipid droplet formation and maturation that involves coordinated redistribution of multiple PAT proteins. We further report that preexisting pools of these PAT proteins exist prior to substrate loading of adipocytes. These protein pools likely contribute to the capacity of 3T3-L1 adipocytes to accommodate rapid TAG synthesis.

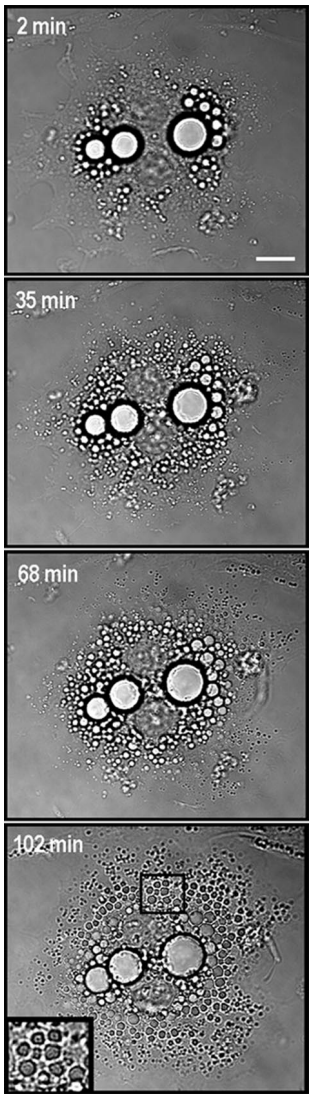

FIG. 1. **Lipid droplets rapidly accumulate during incubation of adipocytes in OGI buffer.** 3T3-L1 adipocytes plated on glass-bottomed dishes were identified and observed in real-time by DIC microscopy during incubation with OGI buffer (1.8 mM oleate). The figure shows a single representative adipocyte at 2, 35, 68, and 102 min after the initiation of OGI treatment. *Bar*, 10 μM.

EXPERIMENTAL PROCEDURES

Reagents—Unless otherwise indicated, reagents were obtained from Sigma. Essentially fatty acid-free bovine serum albumin (BSA) was purchased from Intergen Co. (catalog no: 3320; Purchase, NY).

Fatty Acids—Oleate was solubilized with sodium hydroxide and bound to BSA at a ratio of 5.5 molecules oleate per molecule BSA. BODIPY® FL C_{12} (Molecular Probes, Eugene, OR, catalog no: D3822) was dissolved in dimethyl sulfoxide and bound to BSA at a ratio of 1.4 molecules BODIPY® FL C_{12} per molecule BSA.

Cell Culture—3T3-L1 adipocytes were cultured and differentiated as described previously (10). Day 0 of differentiation was defined as the day by which the 3T3-L1 cells had been confluent for 2 days and were first exposed to the adipogenic mixture that contained 174 nM insulin, 0.25 μM dexamethasone, and 0.5 mM 3-isobutyl-1-methylxanthine. HeLa cells and HIB-1B preadipocytes were grown in Dulbecco's modified Eagle's medium supplemented with 10% fetal bovine serum, 2 mM L-glutamine, 100 units/ml penicillin, and 100 μg/ml streptomycin.

Antibodies—Antibodies to TIP47 were raised in rabbits by Proteintech (Chicago, IL) against the peptide MSSNGTDAPAEAQAAMEEPVC conjugated to keyhole limpet hemocyanin. Antibodies were then affinity purified against this peptide using an antibody purification kit (Pierce, cat. no: 44895) following the manufacturer's protocol. Guinea pig antiserum against adipophilin (11, 12) was purchased from Research Diagnostics Inc. (Flanders, NJ, catalog no: RDI-PROGP40). Rabbit antiserum against calnexin was purchased from Stressgen Biotechnologies Corp. (Victoria, BC, Canada, cat. no. SPA-860). Rabbit antiserum against perilipin (13) was a gift from Constantine Londos. The rabbit antibody and antiserum against the N terminus of S3-12 was described previously (9). Antiserum to mouse Rab GDI-3 was raised against the C-terminal peptide FEEMKRKKNDIYGED by Research Diagnostics, Inc. (Huntsville, AL). Rabbit anti-caveolin-1 was purchased from BD Transduction Laboratories (San Jose, CA, cat. no. C13630).

Isolation of Mouse TIP47 cDNA—The primer set below was used to amplify the full-length coding sequence of mouse TIP47 from a 3T3-L1 adipocyte cDNA library: forward primer, GAAGATCTACCATGTCTAGCAATGGTACAGATGCG; reverse primer, CTCTTTTGGGGACTTCCCTTCATCCGCCGGCGCTTAAGGT. The PCR product was TA-cloned into pCR TOPO2.1 (Invitrogen) and sequenced. The open reading frame that encoded mouse TIP47 was identical to cDNA NM_025836 (14). For mammalian expression, this mouse TIP47 coding sequence was isolated as an EcoRI fragment from pCR TOPO2.1-mouse TIP47 and then subcloned into the EcoRI site of the mammalian expression vector pCAGGS (15), in which expression of the gene of interest is driven by a synthetic promoter based on the chicken β-actin promoter.

Oleate, Glucose, and Insulin (OGI) Treatment—To promote accelerated TAG synthesis, 3T3-L1 adipocytes were grown in complete medium as described (9), washed with phosphate-buffered saline (PBS) (pH 7.4), and then incubated in PBS that contained oleate bound to albumin (see figure legend for concentration), 25 mM glucose, 10 nM insulin, and 2% BSA.

Live Cell Imaging—Day 6 3T3-L1 adipocytes were trypsinized and

replated at 30% their original density into a glass bottom dish. The following day, TAG synthesis was induced by OGI treatment as described above. DIC images were captured every 20 s with a Zeiss LSM 510 Meta laser scanning microscope.

Electron Microscopy—Day 6 3T3-L1 adipocytes were trypsinized and replated at their original density in 35-mm dishes. After 18 h, the adipocytes were either OGI-treated or left untreated for 100 min. Cells were then fixed and prepared for transmission electron microscopy analysis essentially as described (16).

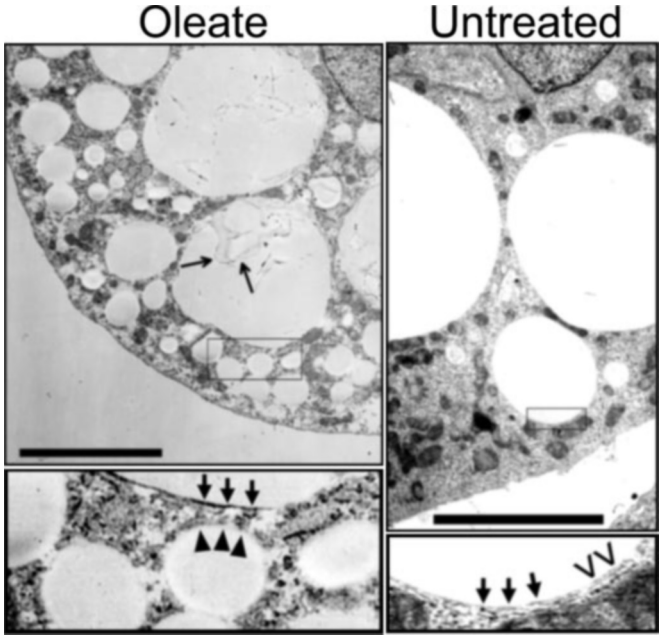

FIG. 2. **OGI-treated adipocytes contain many small (<1 μm) electron-lucent structures.** Quiescent and OGI-treated (1.8 mM oleate) adipocytes were fixed, embedded, and stained for EM. *Solid arrowheads* (▲) point to small, nascent lipid droplets that lack a capsule. The *thick arrows* point to the intact capsule of a large lipid droplet. The *thin arrows* point to detached lipid droplet capsule on a large droplet. *Open arrowheads* point to cisternae that surround large lipid droplets. The enlarged *insets* for the *Oleate* and *Untreated* micrographs are magnified ×4.2 and ×4.6, respectively. *Bars*, 5 μm.

HeLa Cell Transfections—HeLa cells were transfected with 0.5 μg of pCAGGS-mTIP47 plasmid DNA and 7 μl of FuGENE 6 (Roche Applied Science) per 35-mm dish using the manufacturer's protocol.

Generating Fluorescent-labeled HeLa Cell Lipid Droplets—HeLa cells on coverslips were incubated 18 h with 6 μM fluorescent fatty acid BODIPY® FL C_{12} and 225 μM albumin-bound oleate.

Immunoblotting—Cells were washed well with PBS and solubilized with HNETC lysis buffer (50 mM HEPES, pH 7.4, 150 mM NaCl, 2 mM EDTA, and 1% Triton X-100, 0.5% cholate, and Complete protease inhibitors mixture (Roche Applied Science; cat. no: 1 836 153)). A 21,000 × *g* × 10 min supernatant was generated. The solubilized proteins were resolved in Bio-Rad XT precast gels and blotted according to the manufacturer's directions. Membranes were blocked in PBS with 0.1% Tween-20 and 3% BSA. The membranes were then probed with primary antibody in the blocking buffer at the concentrations indicated in the figure legends. The membranes were washed several times in PBS with 0.1% Tween-20 and then incubated with the appropriate horseradish peroxidase-conjugated secondary antibodies in blocking buffer. The membranes were washed again several times in PBS with 0.1% Tween-20. Immunoreactive proteins were detected by enhanced chemiluminescence and imaged with a FluorChem 8900 imager (Alpha Innotech, San Leandro, CA). For quantitation, relative band signals were calculated using AlphaEase FC software (Alpha Innotech, San Leandro, CA).

Immunofluorescence Microscopy—Day 6 or 7 3T3-L1 adipocytes were trypsinized and replated onto coverslips at one-third their original density. The following day, adipocytes were treated as described in the figure legends. The adipocytes were then fixed, stained with antibody dilutions as noted in the figure legends, and imaged as described previously (9).

Fractionation of 3T3-L1 Adipocytes—The following procedure was performed as rapidly and as close to 4 °C as possible. Four 100-mm plates of Day 7 3T3-L1 adipocytes were scraped in PBS and centrifuged at 3220 × *g* for 180 s. The adipocyte pellets were resuspended in 1 ml of lysis buffer (10 mM HEPES-NaOH, pH 7.3, 1 mM EDTA). Adipocytes were allowed to swell for 10 min and then were disrupted by nitrogen cavitation (600 psi for 15 min) in a Parr Cell Disruption Bomb, model

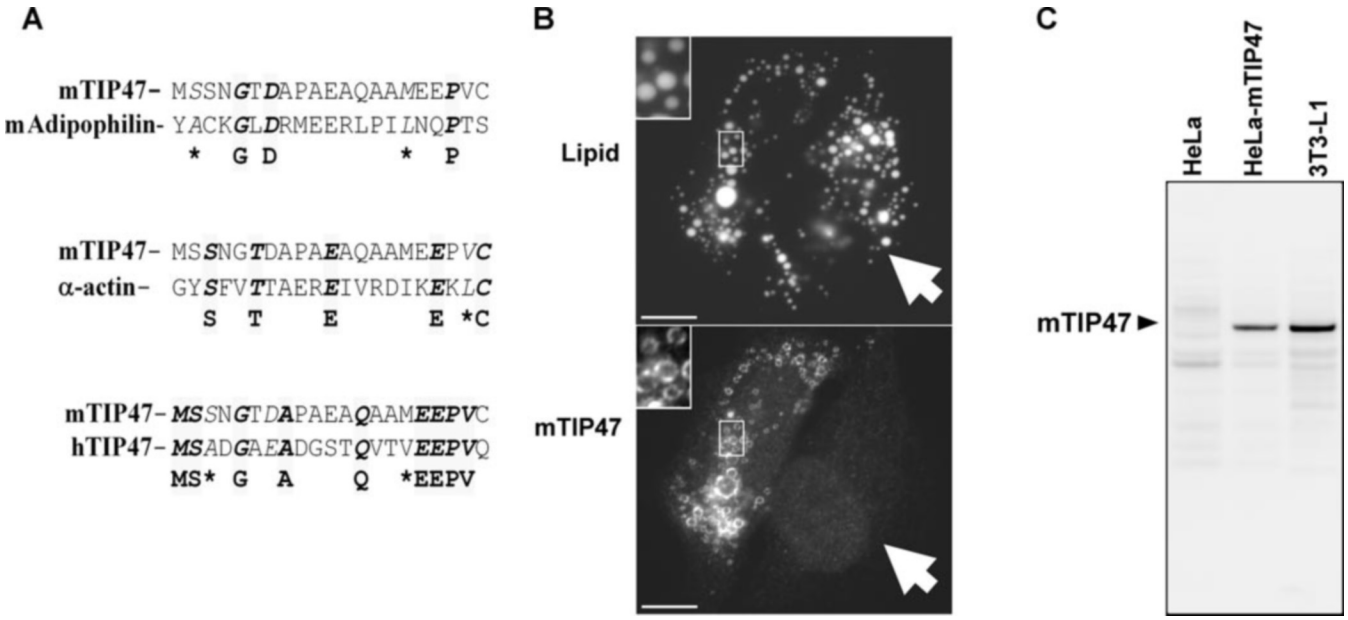

FIG. 3. **Antibody raised against mouse TIP47 coats lipid droplets in HeLa cells transfected with mouse TIP47.** *A*, mouse TIP47 immunizing peptide shares no epitopes with mouse adipophilin. This panel shows the best alignments found by *CLUSTAL* (23) between the immunizing peptide and the proteins mouse adipophilin, α-actin, and human TIP47. Note that sequence identity between mouse TIP47 (mTIP47) and mouse adipophilin is no greater than that between mTIP47 and the completely unrelated protein α-actin. An *asterisk* (*) indicates a structurally conservative amino acid difference. *B*, exogenously expressed mouse TIP47 associates with lipid droplets in HeLa cells. HeLa cells grown on glass coverslips were transfected with pCAGGS-mTIP47. Fluorescent lipid droplets were generated by incubating the cells with both fluorescent fatty acid and oleate as described under "Experimental Procedures." Cells were then fixed and probed with anti-TIP47 at 400 ng/ml. The *white arrow* points to an untransfected HeLa cell. *Bars*, 10 μm. *C*, TIP47 antibody specifically recognizes mouse TIP47. Proteins from untransfected HeLa cells, HeLa cells transfected with pCAGGS-mTIP47, and Day 8 3T3-L1 adipocytes were resolved by PAGE, blotted, and probed with anti-TIP47 at 400 ng/ml.

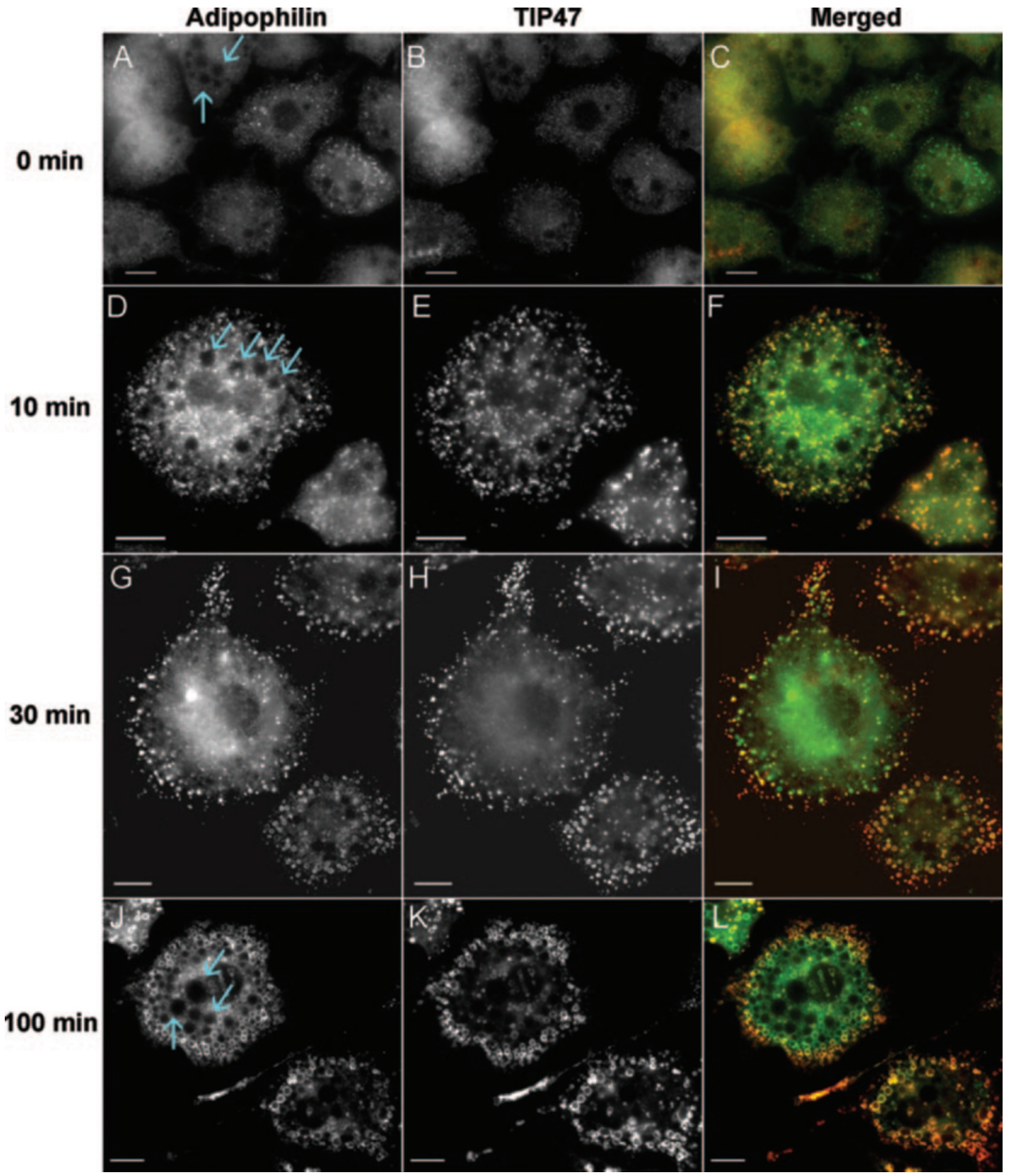

FIG. 4. **TIP47 and adipophilin coat lipid droplets in response to OGI.** Day 6 3T3-L1 adipocytes were trypsinized and replated at 30% their original density onto coverslips. After 18 h, the adipocytes were treated for the times indicated with OGI buffer (900 μM oleate). Then the adipocytes were stained with adipophilin antiserum diluted 1:250 and anti-mouse TIP47 at 300 ng/ml. *Panels A*, *D*, *G*, and *J* show adipophilin staining and *panels B*, *E*, *H*, and *K* show TIP47 staining. The merged images (*panels C*, *F*, *I*, and *L*) show staining for adipophilin protein in *green* and TIP47 protein in *red*. Overlap of adipophilin and TIP47 staining is shown in *yellow*. *Blue arrows* point to selected large lipid storage droplets. *Bars*, 10 μm.

4639 (Parr Instruments Company, Moline, IL). The resulting homogenate was centrifuged at 1000 × *g* for 10 min. 1 ml of the supernatant was collected and weighted with 1.5 ml of 65% sucrose (w/w). 2 ml of weighted supernatant were pipetted into a 5-ml centrifuge tube. Then 1.1-ml layers of 30% followed by 10% sucrose (w/w) in lysis buffer were layered on top of the sucrose supernatant. The tube was filled to capacity with lysis buffer. The gradients were centrifuged at increasing forces: 5 min at 2700 × *g*, 10 min at 10,700 × *g*, 20 min at 43,000 × *g*, 30 min at 172,000 × *g* and then allowed to coast to a stop. The floating fraction was visualized as a white layer at the top of the gradient and was isolated by cutting the tube with a tube slicer (Beckman Coulter, Inc., Fullerton, CA) just below the floating fraction. This fraction was brought to 650 μl with lysis buffer. Then 7 additional 650-μl fractions were collected.

Cycloheximide Treatment—Cycloheximide was added from a 100 mg/ml stock dissolved in dimethyl sulfoxide to a final concentration of 100 μg/ml.

TAG Measurements—Gradient fractions were added directly to the colorimetric TAG quantitation reagent (Wako Chemicals USA, Inc., Richmond, VA, cat. no. L-Type TG H). Corn oil dissolved in ethanol was used as a TAG standard.

TAG Measurement to Assess TAG Synthesis Rates—Approximately 2% of a Day 5 or Day 6 100-mm plate of 3T3-L1 adipocytes were plated in each well of a 24-well plate. On Day 7, adipocytes were treated as described in the legend of Fig. 7. Then TAG was extracted as described previously (17). The lipid phases were dried, and the colorimetric TAG quantification reagent (Thermo Electron Corporation, Melbourne, Australia, cat. no. 2780-400H) was added to the lipid residue. The corn oil standard was added before the extraction and processed with the samples.

Protein Extraction from Mouse Adipose Tissue—Protein was extracted from epididymal fat pads of C57BL/6 mice as described (9) and as approved by the Animal Care Committee of Washington University.

RESULTS

Real-time DIC Microscopy of 3T3-L1 Adipocytes during Active TAG Synthesis—We have previously shown that 3T3-L1 adipocytes rapidly accumulate TAG in oleate-supplemented

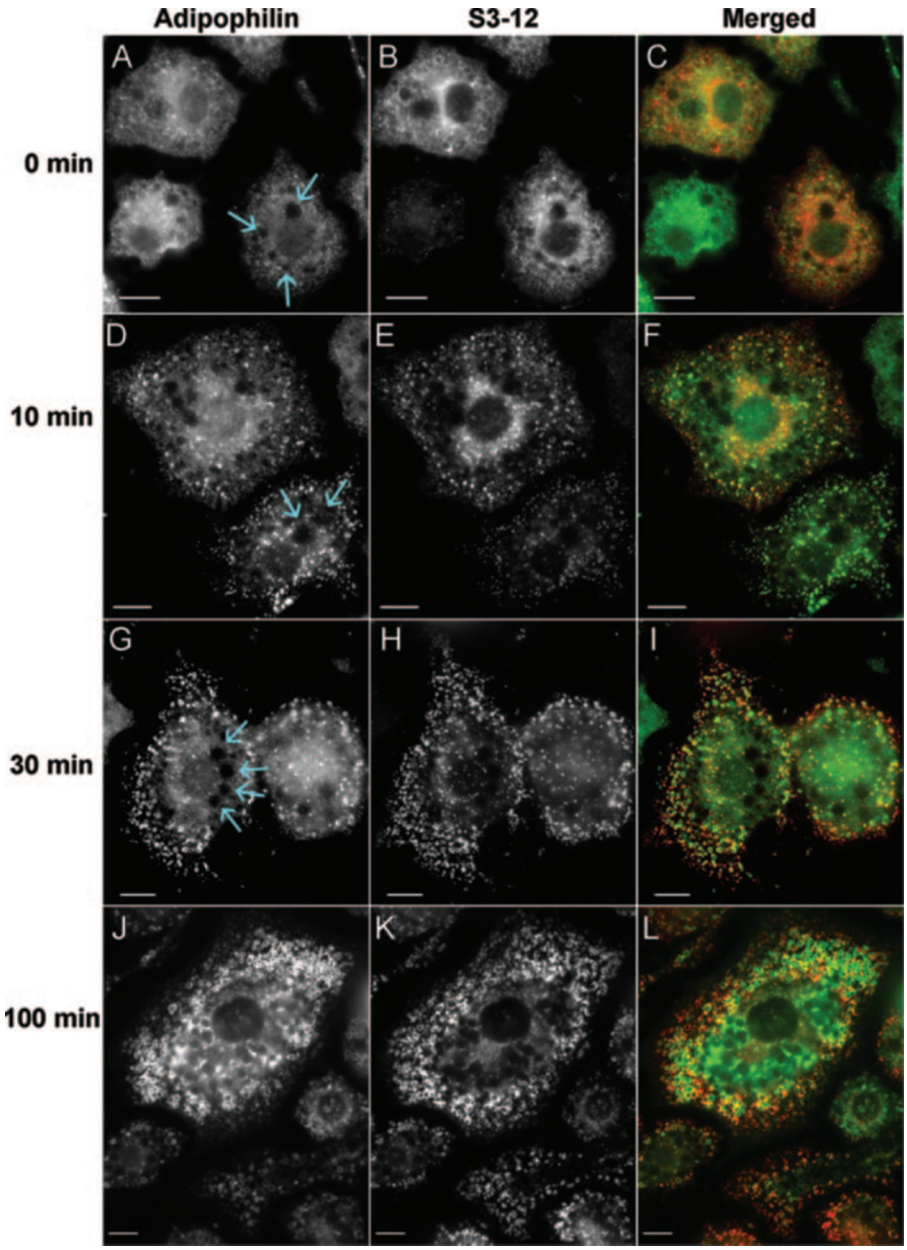

FIG. 5. **After OGI treatment, S3-12 is found on lipid droplets that are peripheral to adipophilin-coated lipid droplets.** 3T3-L1 adipocytes on coverslips were treated for the times indicated with OGI buffer (900 μM). Then the adipocytes were stained with antiserum to adipophilin diluted 1:250 and antibodies to S3-12 at 800 ng/ml. *Panels A*, *D*, *G*, and *J* show adipophilin staining and *panels B*, *E*, *H*, and *K* show the S3-12 staining. The merged images (*panels C*, *F*, *I*, and *L*) show staining for adipophilin protein in *green* and S3-12 protein in *red*. Overlap of adipophilin and S3-12 staining is shown in *yellow*. *Blue arrows* point to selected large lipid storage droplets. *Bars*, 10 μm.

medium and that during rapid TAG accumulation S3-12 moves from a diffuse distribution onto nascent lipid droplets. These nascent lipid droplets increase in size during continued incubation with oleate. Our previous microscopy showed fixed adipocytes, and thus the dynamic process of lipid droplet biogenesis has not been examined. For example, it is unclear whether these nascent lipid droplets grow by fusion with other nascent droplets or by synthesis of new TAG. Lipid droplets in 3T3-L1 adipocytes can be identified by DIC microscopy as well-defined, translucent, spherical structures of ~0.5–10 microns diameter. In order to detect changes in the lipid droplets of adipocytes in real-time, we treated live 3T3-L1 adipocytes with OGI to promote rapid TAG synthesis and captured DIC images at 20-s intervals. Adipocytes were identified by their characteristic round shape and numerous lipid droplets. Under basal culture conditions (Dulbecco's modified Eagle's medium with 10% fetal bovine serum), lipid droplets were arranged with the smallest droplets at the periphery and the largest droplets in the thick, perinuclear region of the adipocyte. The lipid droplets were usually present in clusters or rows rather than being evenly distributed throughout the cytosol. Over the 102 min of the experiment, the lipid droplets maintained their clustered arrangement with the smallest lipid droplets at the adipocyte periphery and the larger lipid droplets near the nuclei (Fig. 1).

The most obvious morphological change in the adipocyte during OGI incubation was a large increase in the size and number of small and medium-sized lipid droplets (<2-μm diameter). Observations at 20-s intervals over 102 min failed to document any clear fusion events between lipid droplets. Smaller, peripheral droplets enlarged and migrated centrally. By 68 min the adipocyte cytoplasm had become filled with lipid droplets and the perinuclear lipid droplets were packed tightly. Because of the large number and rapid movements in three dimensions of the perinuclear lipid droplets, combined with relatively long periods between frames, fusion events may have gone undetected.

Nascent and Mature Lipid Droplets Observed by Transmission Electron Microscopy—To assess ultrastructural changes that occur in adipocytes during rapid TAG synthesis, we analyzed OGI and untreated adipocytes by TEM. Both the OGI and untreated adipocytes contained multiple round, electron-lucent voids (>1-micron diameter). In the untreated adipocytes, these

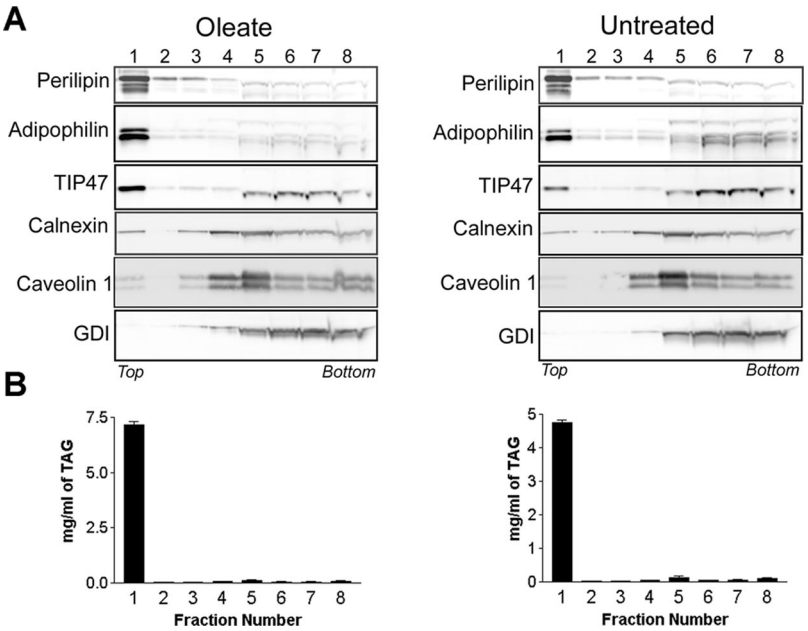

FIG. 6. **Perilipin, TIP47, and adipophilin fractionate with TAG in 3T3-L1 adipocytes.** 3T3-L1 adipocytes were fractionated in a bottom-loaded sucrose gradient as described under "Experimental Procedures," either after 100 min of incubation in 1.8 mM albumin-bound oleate (*Oleate*) or without such incubation (*Untreated*). *A* shows immunoblots with 15 μl of PAGE-resolved proteins from each gradient fraction. Each immunoblot was probed with the antibody indicated in the figure. *B* shows bar graphs that indicate the concentration of TAG in each 650-μl fraction from oleate-treated and untreated adipocytes (n = 3, *error bars*, S.E.).

voids were usually surrounded by cisternae that appeared as tubules in thin sections. An electron dense capsule was apparent at the periphery of some of the void structures, where breaks occurred during processing (Fig. 2). These electron-lucent voids have been identified previously as lipid droplets surrounded by ER (18, 19) and coated by perilipin (19). In OGI-treated adipocytes, there are many small electron lucent voids (<1-micron diameter) in addition to the large cisternae-blanketed lipid droplets. These voids were not surrounded by any observable capsule and were largely found at the periphery and base of the adipocytes. Like the nascent lipid droplets observed by DIC microscopy, the small electron-lucent voids usually formed rows or clusters. The size, location, time of appearance, and organization of the small electron-lucent structures suggest that they correspond to the OGI-induced nascent lipid droplets originally identified by fluorescence and DIC microscopy. Notably, in OGI-treated adipocytes, we identified no physical association of nascent lipid droplets with ER membranes, and we visualized no "lens" structures associated with ER membranes.

A Polyclonal Antibody Specifically Recognizes TIP47 in 3T3-L1 Adipocytes—In non-adipocytes, the PAT protein TIP47 has been reported to coat lipid droplets (7, 8, 20–22). In order to assess whether TIP47 protein is expressed in adipocytes and whether OGI treatments affect the subcellular distribution of TIP47, we raised an anti-peptide antibody to the N-terminal 20 residues of mouse TIP47. We chose this epitope because it has no significant amino acid conservation with mouse adipophilin as assessed by Clustal (23) (Fig. 3*A*). Further, the N terminus of TIP47 is poorly conserved between the mouse and human, which allowed generation of an antibody that recognized mouse TIP47, but not adipophilin or human TIP47. Proteins extracted from untransfected HeLa cells, from HeLa cells expressing mouse TIP47, and from 3T3-L1 adipocytes were resolved by PAGE and blotted. As expected, the TIP47 antibody reacts strongly with a single species from HeLa cells transfected with mouse TIP47 (Fig. 3*B*) and shows little reactivity against proteins in untransfected HeLa cells. The most prominent band detected by our mouse TIP47 antibody is consistent with the predicted molecular weight of TIP47. Faint bands were visualized in all 3 samples, and likely represented nonspecific antibody binding. Further, in 3T3-L1 adipocytes, this antibody recognizes a polypeptide that co-migrates with the major immunoreactive species in HeLa cells transfected with mouse TIP47 (Fig. 3*B*). Immunofluorescence microscopy using this antibody shows only a faint, diffuse signal in untransfected, lipid-loaded HeLa cells (Fig. 3*C*, anti-TIP47, cell on right indicated with *white arrow*). However, in HeLa cells that express mouse TIP47, this antibody strongly labels the surfaces of lipid droplets (Fig. 3*C*, anti-TIP47, cell on left). These data demonstrate that the TIP47 antibody that we have generated specifically recognizes native mouse TIP47. Furthermore, the immunostaining shows unmodified TIP47 on the surface of lipid droplets. This finding is consistent with a similar study, in which human TIP47 expressed in mouse cells was demonstrated to coat lipid droplets (22).

The Dynamics of PAT Protein Distribution during Active TAG Synthesis—The rapid redistribution of S3-12 to the surface of nascent lipid droplets during oleate loading of 3T3-L1 adipocytes (9) led us to hypothesize that the PAT proteins TIP47 and adipophilin also move in response to accelerated TAG synthesis. To assess roles of TIP47 and adipophilin in the genesis of nascent lipid droplets, we stained untreated and OGI-treated adipocytes with either TIP47 antibodies and adipophilin antiserum or S3-12 antibodies and adipophilin antiserum (11, 12). We found that both TIP47 and adipophilin staining patterns were diffuse in untreated adipocytes (Fig. 4, *panels A* and *B*). At 10 min of OGI treatment, S3-12, TIP47, and adipophilin were found in a largely overlapping distribution on small, peripheral lipid droplets at the base of the adipocytes near the coverslip (Figs. 4 and 5, *panels D–F*). At 30 min of OGI treatment, TIP47 and S3-12-coated lipid droplets that formed a ring at the periphery of the adipocyte. At the same time, adipophilin formed a concentric ring of larger lipid droplets that largely overlapped the S3-12 and TIP47 coated droplets, but was centered closer to the nucleus (Figs. 4 and 5, *panels G–I*). Even at 100 min, TIP47 remained almost completely separate from the large central droplets, whereas S3-12 and adipophilin can be found on large central droplets (Figs. 4 and 5, *panels J–L*).

OGI Treatment Drives TIP47 and Adipophilin into the Lipid Droplet Fraction—To biochemically assess the effect of OGI-driven TAG synthesis on the cellular distribution of PAT proteins and to better understand the source of the S3-12, TIP47 and adipophilin on nascent lipid droplets, untreated and OGI-treated 3T3-L1 adipocytes were disrupted by nitrogen cavita-

tion and fractionated on density gradients. Blotted gradient fractions were probed with antibodies that recognized a Rab guanine-nucleotide dissociation inhibitor (GDI), calnexin, and perilipin in order to identify fractions enriched in cytosol, membranes, and lipid droplets, respectively (Fig. 6). Lipid droplet-enriched fractions were confirmed by assay for triacylglycerol. Most perilipin protein and almost all TAG floated to the top of the gradient in fraction 1. Peak immunoreactivities to the membrane proteins calnexin and caveolin-1 were in the middle of the gradient (fraction 5). Immunoreactivity to the soluble protein marker Rab GDI was distributed evenly in the bottom 3 fractions (fractions 6–8) with less intense signals in fractions 4 and 5. Consistent with previous studies of non-adipocytes (8, 24, 25), in untreated 3T3-L1 adipocytes most TIP47 was found at the bottom of the density gradient with the cytosolic marker. In contrast, in oleate-treated 3T3-L1 adipocytes, much of the TIP47 was found at the top of the density gradient in fraction 1 with the lipid droplet marker perilipin and TAG. These data are consistent with our immunofluorescence microscopy data that show TIP47 moving from a diffuse cellular distribution to the surfaces of lipid droplets during OGI-treatment. This OGI-induced movement of TIP47 from the cytosol onto lipid droplets has been previously reported to occur in non-adipocytes (8). In both untreated and OGI-treated adipocytes, much of the adipophilin is in the floating, perilipin-rich fractions. Like TIP47, OGI-treatment causes an increase in the portion of adipophilin that fractionates with the lipid droplet markers. This observation is consistent with our immunofluorescence microscopy, which shows adipophilin moving from a diffuse distribution to the surface of lipid droplets in adipocytes. The adipophilin in the perilipin-rich fraction of untreated 3T3-L1 cells likely reflects the basal distribution of adipophilin in incompletely differentiated adipocytes, in which adipophilin coats lipid droplets under basal conditions (13). In fact, we observe adipophilin on small lipid droplets in post-differentiation 3T3-L1 cells that lack large lipid droplets (data not shown).

In our hands only a small and variable fraction of total cellular S3-12 is recoverable following lysis of adipocytes in the absence of detergents, as is required for lipid droplet fractionation. Thus, we were unable to assess the distribution of S3-12 biochemically by our lipid droplet fractionation technique.

Caveolin proteins or caveolin mutants have been reported to associate with lipid droplets and have been implicated in lipid droplet biogenesis (26, 27). In order to address the possibility of caveolin proteins being a component of the coat of these newly described lipid droplets, we assessed the distribution of caveolin in the fractions of untreated and OGI-treated adipocytes. We found that caveolin-1 distribution was very similar to that of the membrane marker calnexin. Further, the caveolin distribution was unaffected by oleate treatment (Fig. 6). These results were consistent with our immunofluorescence observations, in which caveolin-1 was found on the plasma membrane and on intracellular puncta, but not on lipid droplets under either untreated or OGI-treated conditions (data not shown).

New Protein Synthesis Is Not Required for the Generation of Nascent PAT Protein-coated Lipid Droplets or for TAG Storage—We have shown that nascent lipid droplets coated with PAT proteins emerge within 30 min of adding OGI. The diffuse cytoplasmic staining for S3-12, TIP47, and adipophilin that we have observed under basal conditions fails to clarify whether the PAT proteins that coat nascent droplets are newly synthesized or are recruited from preexisting pools. To investigate this question, we added albumin-bound oleate to 3T3-L1 adipocytes in the presence or absence of cycloheximide, an inhibitor of protein synthesis. At 30 min of incubation we assessed the generation of PAT protein-coated nascent droplets by im-

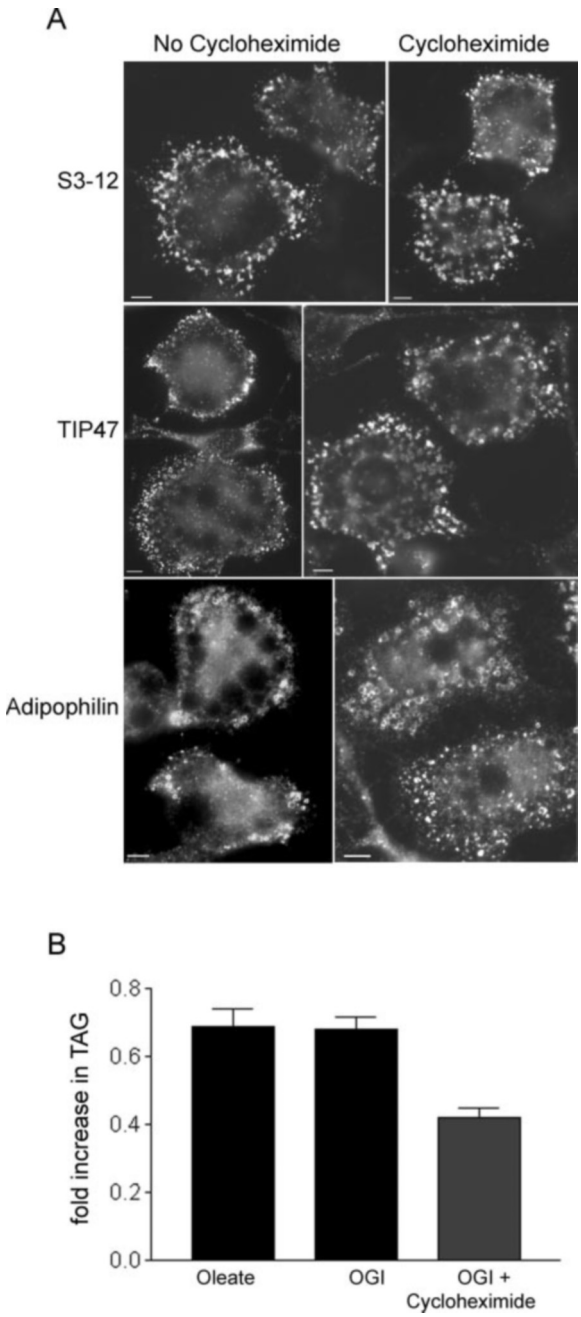

FIG. 7. **Cycloheximide does not inhibit TIP47, S3-12, and adipophilin redistribution or block TAG accumulation.** *A*, 3T3-L1 adipocytes on coverslips were pretreated with OGI medium lacking oleate and where indicated with 100 μg/ml cycloheximide. After 10 min, albumin-bound oleate was added to the OGI medium to a final concentration of 1.8 mM. After 30 min the 3T3-L1 adipocytes were fixed and stained with the antibodies or antisera indicated. *Bars*, 10 μm. *B*, 3T3-L1 adipocytes on coverslips were treated as follows. *Oleate*, adipocytes were incubated for 3 h in normal culture medium supplemented with albumin-bound oleate to a final concentration of 1.8 mM. *OGI*, 3T3-L1 adipocytes were pretreated with OGI medium lacking oleate. After 10 min, albumin-bound oleate was added to the OGI medium to a final concentration of 1.8 mM. Adipocytes were incubated for an additional 3 h. *OGI + Cycloheximide*, adipocytes were treated as above for *OGI* except 100 μg/ml cycloheximide was added to the pretreatment buffer. TAG was then measured in the adipocytes as described above and also in untreated adipocytes to determine baseline TAG levels. Fold increase in TAG was calculated by dividing the amount of TAG in the treated adipocytes by the amount of TAG in the untreated. The data shown are from two experiments, each with 12 replicates. The amount of TAG in all three treatments with oleate differed significantly ($p < 0.01$) from the TAG in adipocytes not treated with oleate. Amounts of TAG in the Oleate- and OGI-treated adipocytes differed significantly ($p < 0.01$) from the TAG in the OGI + Cycloheximide-treated adipocytes.

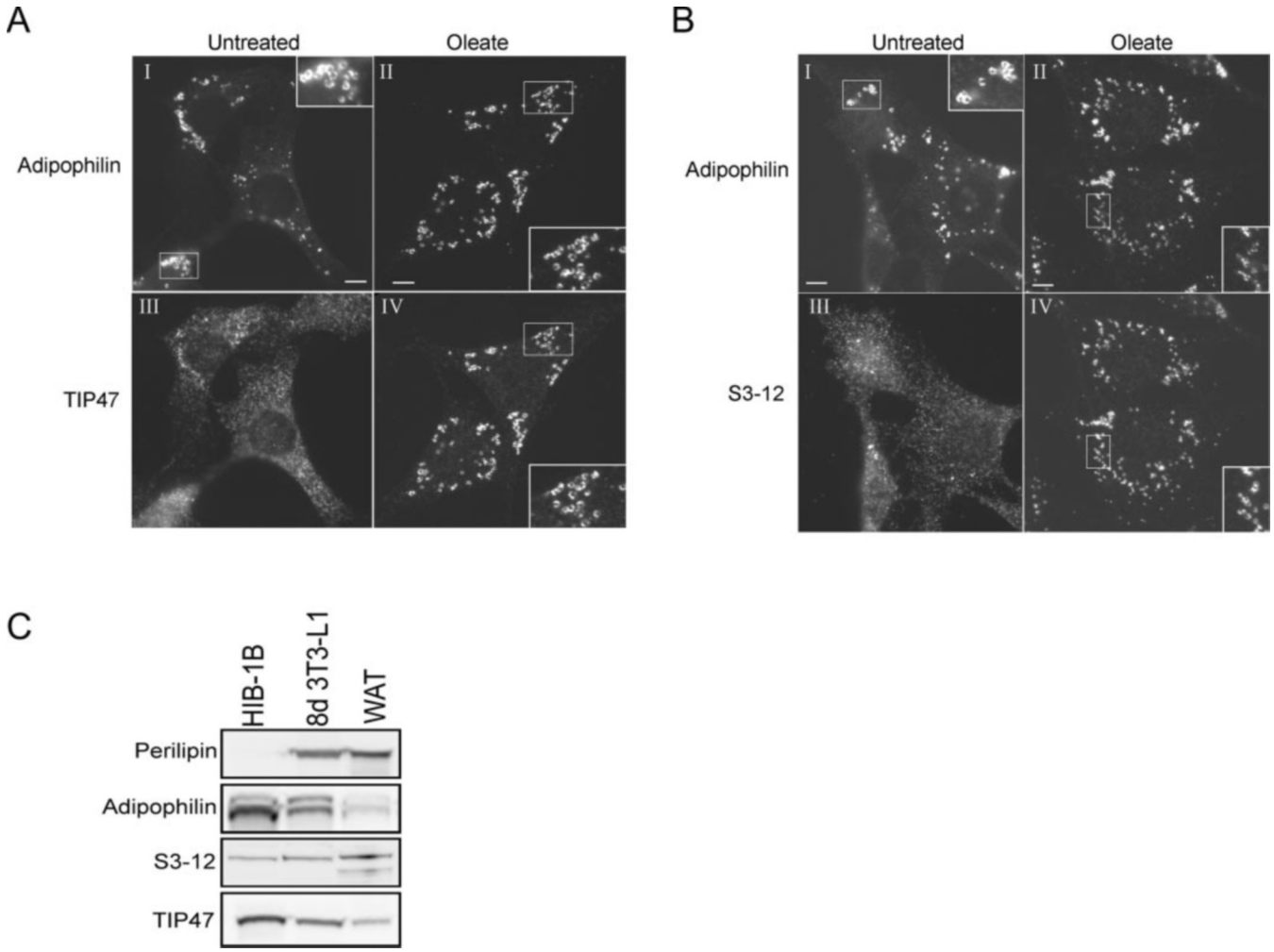

FIG. 8. **S3-12 and TIP47 in preadipocytes move to adipophilin-coated lipid droplets with oleate treatment.** HIB-1B preadipocytes were grown to 50% confluence on coverslips. *A* and *B*, panels labeled *Oleate* indicate the cells were treated with 450 μM albumin-bound oleate for 2 h. All cells were stained with antiserum to adipophilin diluted 1:500. *A* also shows cells stained with TIP47 antibodies at 400 ng/ml. *B* shows cells that are also stained with antibodies to S3-12 at 2.4 μg/ml. *Bars*, 10 μm. *C* shows PAGE-resolved blotted proteins from HIB-lB cells, Day 8 3T3-L1 adipocytes and mouse white adipose tissue (*WAT*) probed with perilipin antiserum (1:5,000), anti-adipophilin (1:1,000), S3-12 antiserum (1:2000), and anti-TIP47 (640 ng/ml) as indicated.

munofluorescence microscopy. The appearance of lipid droplets coated with S3-12, TIP47, or adipophilin was not blocked when new protein synthesis was inhibited by cycloheximide (Fig. 7).

Our adipocyte cell fractionation studies suggested that the total amount of S3-12, TIP47, and adipophilin does not differ significantly in oleate-treated *versus* untreated adipocytes. To assess this point further, we immunoblotted proteins resolved from unfractionated adipocytes either treated with oleate for 30 min or not treated with oleate, and then we quantified relative expression of the PAT proteins by densitometry. We found that 30 min of oleate treatment was associated with no statistically significant changes in expression of PAT proteins. Specifically, S3-12 protein decreased by 3.6% with a S.D. of 13%, TIP47 increased by 2.6% with a S.D. of 21%, adipophilin increased by 4.5% with a S.D. of 19%, and perilipin decreased by 7.5% with a S.D. of 17% ($n = 4$).

The observation that inhibiting protein synthesis does not block the emergence of nascent lipid droplets led us to hypothesize that the ability of adipocytes to package, store, and accumulate TAG acutely in response to lipid loading does not require new protein synthesis. To test this hypothesis, we drove TAG synthesis in adipocytes with OGI or oleate-supplemented medium. To limit protein synthesis, we treated adipocytes with cycloheximide in OGI medium that lacked amino acids. After prolonged (3 h) incubation adipocytes incubated in either OGI buffer or oleate-supplemented medium accumulated almost 70% more TAG than untreated cells. Adipocytes incubated in OGI with cycloheximide accumulated about one-third less TAG than adipocytes incubated in OGI alone (Fig. 7*B*).

Intermediate Pools of Lipid Droplets Are Specific to Adipocyte—For reasons of convenience, most cell biology experiments utilize fast growing, immortalized cell lines grown in lipid-poor medium. Under these conditions, non-adipocytes have only small rare and transient lipid droplets (8, 28, 29). In order to assess how the PAT proteins behave in non-adipocytes, we utilized HIB-1B preadipocytes, which can be differentiated into brown adipocytes. As preadipocytes, these cells have stable lipid droplets when grown in standard lipid-poor medium and express S3-12, TIP47, and adipophilin, but not perilipin as assessed by immunoblot (Fig. 8*C*). Thus, HIB-1B preadipocytes allow the study of endogenous S3-12, TIP47, and adipophilin in non-adipocytes. Furthermore, the preexisting lipid droplets raise the possibility of generating a population of nascent droplets. In HIB-1B preadipocytes grown in lipid-poor medium, adipophilin is found on lipid droplets, but TIP47 and S3-12 are distributed diffusely, as we have described in untreated 3T3-L1 adipocytes. When HIB-1B preadipocytes are incubated with oleate, the size and number of lipid droplets increase, and these

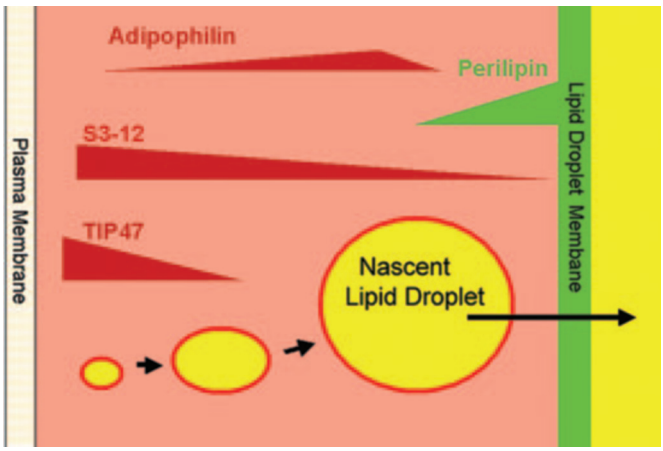

FIG. 9. **Model of lipid droplet maturation in adipocytes.** Our data are consistent with a model of lipid droplet biogenesis in which the composition of the lipid droplet PAT protein coat changes as small, nascent droplets enlarge and move centrally toward the large perilipin-coated storage droplets.

droplets become coated with S3-12 and TIP47 (Fig. 8). Unlike adipocytes, oleate treatment drives TIP47 and S3-12 onto the existing adipophilin-coated droplets, and thus does not result in the multiple populations of droplets seen in 3T3-L1 adipocytes (Figs. 4 and 5).

DISCUSSION

In previous work we reported that the PAT protein S3-12 coats nascent lipid droplets during accelerated TAG synthesis in 3T3-L1 adipocytes (9). These droplets were distinct from the perilipin-coated storage droplets. Our current data extend these observations to show 1) that nascent lipid droplets form peripherally and move toward the perinuclear storage droplets, 2) that nascent droplets enlarge as they move centrally, perhaps by synthesis of new TAG directly in the droplet rather than by droplet fusion, 3) that the protein coat of nascent droplets changes as they move centrally over time, and 4) that the PAT proteins are recruited to the nascent droplet surface from preexisting pools. That we did not observe fusion events between nascent droplets is consistent with previous imaging of lipid droplet formation in live Vero cells (30). The lack of frequent fusion events suggests the possibility that nascent lipid droplets enlarge by addition of TAG into the droplets, perhaps by synthesis of TAG on the droplets themselves. Consistent with this notion is the finding of multiple forms of acyl-CoA synthase, the enzyme required to activate long chain fatty acids for TAG synthesis, in lipid droplet enriched fractions from several cell types including adipocytes (20, 31, 32). Furthermore, DGAT activity fractionates with lipid droplets in *Saccharomyces cerevisiae* (33).

Our data do not address whether nascent lipid droplets eventually dock and fuse with the perinuclear lipid storage droplets coated by perilipin. We have observed previously that by 240 min of lipid loading, S3-12 moves onto the perinuclear, perilipin-coated lipid droplets (9). In the current study adipophilin staining appears on at least some perinuclear droplets at 100 min of lipid loading. These data suggest that physical communication between the nascent droplets and the mature perilipin-coated lipid droplets takes place, whether actual droplet fusion occurs or not. Our data do not address whether late fusion events after 100 min occur.

Our ultrastructural study showed that adipocytes treated with OGI amassed many small lipid droplets that lacked both the surrounding ER-cisternae and the droplet capsule (Fig. 2). We and others (18, 19) have observed such structures around most lipid droplets in untreated adipocytes, and we have observed them around large lipid droplets in OGI-treated adipocytes. Given a prevailing model of lipid droplet biogenesis, which holds that lipid droplets originate from the ER membrane bilayer, our findings are surprising and suggest that adipocyte lipid droplets, at least those derived from exogenous fatty acids may originate from specialized structures other than the ER. It is also possible that, under the conditions of our experiment, the nascent droplets budded off from the ER too rapidly for detection in the ER-associated state. In any event, our data do not support a persistent association of nascent droplets with the ER membrane.

Co-staining for PAT proteins demonstrated what appeared by immunofluorescence to be preexisting pools of S3-12, TIP47 and adipophilin distributed diffusely throughout the adipocyte under basal conditions. These results were expected for both S3-12 and TIP47, because of prior work showing by immunoblot expression of S3-12 in non-lipid loaded 3T3-L1 adipocytes (9) and of TIP47 in HeLa and MA-10 Leydig cells (8). However, adipophilin has been reported as exclusively or almost exclusively associated with lipid droplets in non-adipocytes (24, 34, 35). We also find this to be the case in HIB-1B preadipocytes (Fig. 8). However, three observations suggest that 3T3-L1 adipocytes have a soluble pool of adipophilin that is not associated with lipid droplets. First, significant adipophilin is found in cytosolic fractions of 3T3-L1 adipocytes (Fig. 6*A*). Second, inhibition of protein synthesis does not inhibit the emergence of adipophilin-coated lipid droplets (Fig. 7*A*). Third, adipophilin-coated lipid droplets emerge without a significant change in the total amount of adipophilin, as reported under "Results." If our finding of OGI-induced coating of lipid droplets with adipophilin were caused by synthesis of new adipophilin, then we would have expected to measure a significant increase in immunoreactive adipophilin protein associated with appearance of such droplets. Due to poor recovery of S3-12 out of our isolated cell fractions, we lack data to determine whether the basal pool of S3-12 is soluble or membrane-associated. Nevertheless, our data support a model of lipid droplet coat formation in which soluble or membrane-associated proteins are recruited to the surfaces of nascent droplets by protein-protein interactions or, more likely, by the increased availability of hydrophobic surfaces on the nascent droplets.

A structural basis for how PAT proteins may be in either soluble or lipid droplet-associated states has been suggested by the recently reported crystal structure of a TIP47 carboxyl polypeptide (36). This polypeptide has a 4 helix bundle similar to that of apoE and conserved between TIP47, S3-12, and adipophilin. In apoE the 4 helices are stable in solution when bundled together. However, the helices can open to expose hydrophobic residues that bind the lipid surface of lipoproteins (37). The PAT proteins and certain exchangeable lipid-binding proteins, such as apoE and α-synuclein, also share an 11-mer repeat motif that has been proposed to form amphipathic helices capable of wrapping around the hydrophobic surface of lipid droplets (38). The presence of hydrophobic interaction interfaces with lipid may explain why the PAT proteins resist extraction from lipid droplets by strong alkali buffers (32). Mechanisms by which PAT proteins bind to lipid droplets will be an important area for future studies.

It remains unknown what specific role each PAT protein plays in the biogenesis of nascent lipid droplets. Our data reveal, however, an ordered process of lipid droplet movement, enlargement, and protein coating that varies as a function of time and subcellular location (Fig. 9). To our knowledge, no previous models of lipid droplet biogenesis have predicted the dramatic changes in the protein coat of the nascent droplets that we now report. Our data make clear that this process in

adipocytes is qualitatively different from that in non-adipocytes, such as HIB-1B preadipocytes. HIB-1B preadipocytes express native S3-12, TIP47, and adipophilin, but do not generate the heterogeneous population of nascent droplets that develop in 3T3-L1 adipocytes during OGI treatment (Fig. 8). Thus, conclusions about the nature of lipid droplet formation and maturation in adipocytes should not be made casually from data obtained in other cell types and organisms.

Acknowledgments—We thank Wandy Beatty of the Washington University Molecular Microbiology Imaging Facility for assistance with live cell microscopy and Marilyn Levy of the Electron Microscopy Facility for preparing samples for and assistance with TEM. We also thank Sheila Collins (Duke University, Durham, NC) for providing HIB-1B pre-brown adipocytes and Constantine Londos (National Institutes of Health, Bethesda, MD) for the perilipin antiserum.

REFERENCES

1. Schaffer, J. E. (2003) *Curr. Opin. Lipidol.* **14,** 281–287
2. Unger, R. H. (2003) *Endocrinology* **144,** 5159–5165
3. Murphy, D. J., and Vance, J. (1999) *Trends Biochem. Sci.* **24,** 109–115
4. Zweytick, D., Athenstaedt, K., and Daum, G. (2000) *Biochim. Biophys. Acta.* **1469,** 101–120
5. Sakashita, N., Miyazaki, A., Takeya, M., Horiuchi, S., Chang, C. C., Chang, T. Y., and Takahashi, K. (2000) *Am. J. Pathol.* **156,** 227–236
6. Quittnat, F., Nishikawa, Y., Stedman, T. T., Voelker, D. R., Choi, J. Y., Zahn, M. M., Murphy, R. C., Barkley, R. M., Pypaert, M., Joiner, K. A., and Coppens, I. (2004) *Mol. Biochem. Parasitol.* **138,** 107–122
7. Miura, S., Gan, J. W., Brzostowski, J., Parisi, M. J., Schultz, C. J., Londos, C., Oliver, B., and Kimmel, A. R. (2002) *J. Biol. Chem.* **277,** 32253–32257
8. Wolins, N. E., Rubin, B., and Brasaemle, D. L. (2001) *J. Biol. Chem.* **276,** 5101–5108
9. Wolins, N. E., Skinner, J. R., Schoenfish, M. J., Tzekov, A., Bensch, K. G., and Bickel, P. E. (2003) *J. Biol. Chem.* **278,** 37713–37721
10. Frost, S. C., and Lane, M. D. (1985) *J. Biol. Chem.* **260,** 2646–2652
11. Heid, H. W., Moll, R., Schwetlick, I., Rackwitz, H. R., and Keenan, T. W. (1998) *Cell Tissue Res.* **294,** 309–321
12. Heid, H. W., Schnolzer, M., and Keenan, T. W. (1996) *Biochem. J.* **320,** 1025–1030
13. Brasaemle, D. L., Barber, T., Wolins, N. E., Serrero, G., Blanchette-Mackie, E. J., and Londos, C. (1997) *J. Lipid Res.* **38,** 2249–2263
14. Strausberg, R. L., Feingold, E. A., Grouse, L. H., Derge, J. G., Klausner, R. D., Collins, F. S., Wagner, L., Shenmen, C. M., Schuler, G. D., Altschul, S. F., Zeeberg, B., Buetow, K. H., Schaefer, C. F., Bhat, N. K., Hopkins, R. F., Jordan, H., Moore, T., Max, S. I., Wang, J., Hsieh, F., Diatchenko, L., Marusina, K., Farmer, A. A., Rubin, G. M., Hong, L., Stapleton, M., Soares, M. B., Bonaldo, M. F., Casavant, T. L., Scheetz, T. E., Brownstein, M. J., Usdin, T. B., Toshiyuki, S., Carninci, P., Prange, C., Raha, S. S., Loquellano, N. A., Peters, G. J., Abramson, R. D., Mullahy, S. J., Bosak, S. A., McEwan, P. J., McKernan, K. J., Malek, J. A., Gunaratne, P. H., Richards, S., Worley, K. C., Hale, S., Garcia, A. M., Gay, L. J., Hulyk, S. W., Villalon, D. K., Muzny, D. M., Sodergren, E. J., Lu, X., Gibbs, R. A., Fahey, J., Helton, E., Ketteman, M., Madan, A., Rodrigues, S., Sanchez, A., Whiting, M., Young, A. C., Shevchenko, Y., Bouffard, G. G., Blakesley, R. W., Touchman, J. W., Green, E. D., Dickson, M. C., Rodriguez, A. C., Grimwood, J., Schmutz, J., Myers, R. M., Butterfield, Y. S., Krzywinski, M. I., Skalska, U., Smailus, D. E., Schnerch, A., Schein, J. E., Jones, S. J., and Marra, M. A. (2002) *Proc. Natl. Acad. Sci. U. S. A.* **99,** 16899–16903
15. Niwa, H., Yamamura, K., and Miyazaki, J. (1991) *Gene* (*Amst.*) **108,** 193–199
16. Shyng, S. L., Heuser, J. E., and Harris, D. A. (1994) *J. Cell Biol.* **125,** 1239–1250
17. Bligh, E. G., and Dyer, W. J. (1959) *Can. J. Biochem. Physiol.* **37,** 911–917
18. Cushman, S. W. (1970) *J. Cell Biol.* **46,** 326–341
19. Blanchette-Mackie, E. J., Dwyer, N. K., Barber, T., Coxey, R. A., Takeda, T., Rondinone, C. M., Theodorakis, J. L., Greenberg, A. S., and Londos, C. (1995) *J. Lipid Res.* **36,** 1211–1226
20. Umlauf, E., Csaszar, E., Moertelmaier, M., Schuetz, G. J., Parton, R. G., and Prohaska, R. (2004) *J. Biol. Chem.* **279,** 23699–23709
21. Than, G. N., Turoczy, T., Sumegi, B., Than, N. G., Bellyei, S., Bohn, H., and Szekeres, G. (2001) *Anticancer Res* **21,** 639–642
22. Ohashi, M., Mizushima, N., Kabeya, Y., and Yoshimori, T. (2003) *J. Biol. Chem.* **278,** 36819–36829
23. Higgins, D. G., and Sharp, P. M. (1988) *Gene* (*Amst.*) **73,** 237–244
24. Barbero, P., Buell, E., Zulley, S., and Pfeffer, S. R. (2001) *J. Biol. Chem.* **276,** 24348–24351
25. Diaz, E., and Pfeffer, S. R. (1998) *Cell* **93,** 433–443
26. Pol, A., Luetterforst, R., Lindsay, M., Heino, S., Ikonen, E., and Parton, R. G. (2001) *J. Cell Biol.* **152,** 1057–1070
27. Ostermeyer, A. G., Paci, J. M., Zeng, Y., Lublin, D. M., Munro, S., and Brown, D. A. (2001) *J. Cell Biol.* **152,** 1071–1078
28. Brasaemle, D. L., Rubin, B., Harten, I. A., Gruia-Gray, J., Kimmel, A. R., and Londos, C. (2000) *J. Biol. Chem.* **275,** 38486–38493
29. Spector, A. A., Mathur, S. N., Kaduce, T. L., and Hyman, B. T. (1980) *Prog. Lipid Res.* **19,** 155–186
30. Pol, A., Martin, S., Fernandez, M. A., Ferguson, C., Carozzi, A., Luetterforst, R., Enrich, C., and Parton, R. G. (2004) *Mol. Biol. Cell* **15,** 99–110
31. Liu, P., Ying, Y., Zhao, Y., Mundy, D. I., Zhu, M., and Anderson, R. G. (2004) *J. Biol. Chem.* **279,** 3787–3792
32. Brasaemle, D. L., Dolios, G., Shapiro, L., and Wang, R. (2004) *J. Biol. Chem.* **279,** 46835–46842
33. Sorger, D., and Daum, G. (2002) *J. Bacteriol.* **184,** 519–524
34. Brasaemle, D. L., Barber, T., Kimmel, A. R., and Londos, C. (1997) *J. Biol. Chem.* **272,** 9378–9387
35. Fujimoto, Y., Itabe, H., Sakai, J., Makita, M., Noda, J., Mori, M., Higashi, Y., Kojima, S., and Takano, T. (2004) *Biochim. Biophys. Acta* **1644,** 47–59
36. Hickenbottom, S. J., Kimmel, A. R., Londos, C., and Hurley, J. H. (2004) *Structure (Camb.)* **12,** 1199–1207
37. Narayanaswami, V., and Ryan, R. O. (2000) *Biochim. Biophys. Acta.* **1483,** 15–36
38. Bussell, R., Jr., and Eliezer, D. (2003) *J. Mol. Biol.* **329,** 763–778